NATIONAL AERONAUTICS AND SPACE ADMINISTRATION

Technical Report 32-1564

An Anechoic Chamber Facility for Investigating Aerodynamic Noise

P. F. Massier

S. P. Parthasarathy

JET PROPULSION LABORATORY

CALIFORNIA INSTITUTE OF TECHNOLOGY

PASADENA, CALIFORNIA

September 15, 1972

NATIONAL AERONAUTICS AND SPACE ADMINISTRATION

Technical Report 32-1564

An Anechoic Chamber Facility for Investigating Aerodynamic Noise

P. F. Massier
S. P. Parthasarathy

JET PROPULSION LABORATORY
CALIFORNIA INSTITUTE OF TECHNOLOGY
PASADENA, CALIFORNIA

September 15, 1972

Preface

The work described in this report was performed by the Propulsion Division of the Jet Propulsion Laboratory.

Acknowledgment

The design and completion of this facility required the services of numerous personnel with special skills and dedication. The authors are deeply grateful to these people for their contributions in making this anechoic chamber a reality, beginning with preliminary discussions and extending to building modifications, preparation of drawings, fabrication, acquisition of surplus materials and equipment, procurement, cost analysis, construction, installation checkout, instrumentation, and, finally, the preparation of this document. In particular, special appreciation is extended to Milton Noel for his enthusiastic participation in virtually all aspects of the project and to Scottie Slover, Stan Kikkert, and Joe Godley for their services associated with the construction, instrumentation, and checkout phases of this effort.

Contents

Tables

Contents (contd)

Tables (contd)

Figures

Contents (contd)

Figures (contd)

Abstract

The aerodynamic noise facility at the Jet Propulsion Laboratory was designed to be used primarily for investigating the noise-generating mechanisms of high-temperature supersonic and subsonic jets. It can, however, be used for investigating other sources of noise as well. The facility consists of an anechoic chamber, an exhaust jet silencer, instrumentation equipment, and an air heater with associated fuel and cooling systems. Compressed air, when needed for jet noise studies, is provided by the wind tunnel compressor facility on a continuous basis.

The chamber is 8.1 m long, 5.0 m wide, and 3.0 m high. Provisions have been made for allowing outside air to be drawn into the anechoic chamber in order to replenish the air that is entrained by the jet as it flows through the chamber. Also, openings are provided in the walls and in the ceiling for the purpose of acquiring optical measurements. Calibration of the chamber for noise reflections from the wall was accomplished in octave bands between 31.2 Hz and 32 kHz.

An Anechoic Chamber Facility for Investigating Aerodynamic Noise

I. Introduction

The aerodynamic noise facility at the Jet Propulsion Laboratory was designed and constructed primarily for the purpose of experimentally investigating the noise generating mechanisms in supersonic and in subsonic jets. It can also be used, however, for investigating many other sources of noise as well. As shown in Fig. 1, the facility consists of an anechoic chamber, a jet exhaust silencer, instrumentation equipment, and an air heater with the associated fuel and cooling systems. Compressed air, when needed for jet noise studies, is supplied on a continuous basis to the air heater by the Wind Tunnel compressor facility.

During operation for the purpose of investigating jet noise, the jet discharges from a nozzle located at one end of the anechoic chamber. As the jet flows through the chamber, a considerable amount of surrounding air is entrained, and hence, the diameter of the jet increases substantially before it leaves the room and enters the exhaust silencer. Measurements of the noise, fluctuating quantities, and fluid-flow quantities are made inside the anechoic chamber. The jet flow is discharged into the atmosphere after it has passed through the silencer. The purpose of the silencer is to absorb most of the noise after the flow has passed through the chamber and thus prevent excessive noise from radiating to the surrounding area.

II. Anechoic Chamber

The anechoic room is constructed of reinforced concrete walls, ceiling and floor, except for one wall shown at the right in Fig. 1, which has an opening for the inlet section of the exhaust silencer. This end of the room consists of a double stud and stucco wall, with a 1.3-m space between the two walls. In the three concrete walls, rectangular openings are located near the ceiling, as shown in Fig. 2, for the purpose of admitting outside air to replenish that which is entrained by the jet. This air is drawn into the room by the small decrease in ambient pressure inside, which is caused by the injector action of the jet. Conventional sound-absorbing panels cover these openings both outside and inside the building to prevent excessive noise from radiating to the surrounding area. The panels are spaced approximately 13 cm from the wall so that the air flows over the tops of the outside panels, through the openings, and around the inside panels, and is then distributed into the room. Figure 3 is a photograph of an outside panel assembly. Sheet-metal covers the tops of these panels to prevent rain from entering the building.

The entire inside surface of the room is lined with fiberglass wedge blocks (Figs. 4 and 5), which were designed for a low-frequency cutoff of 250 Hz. This is significantly below the frequency at which the maximum noise intensity occurs in jets. Furthermore, the intensities

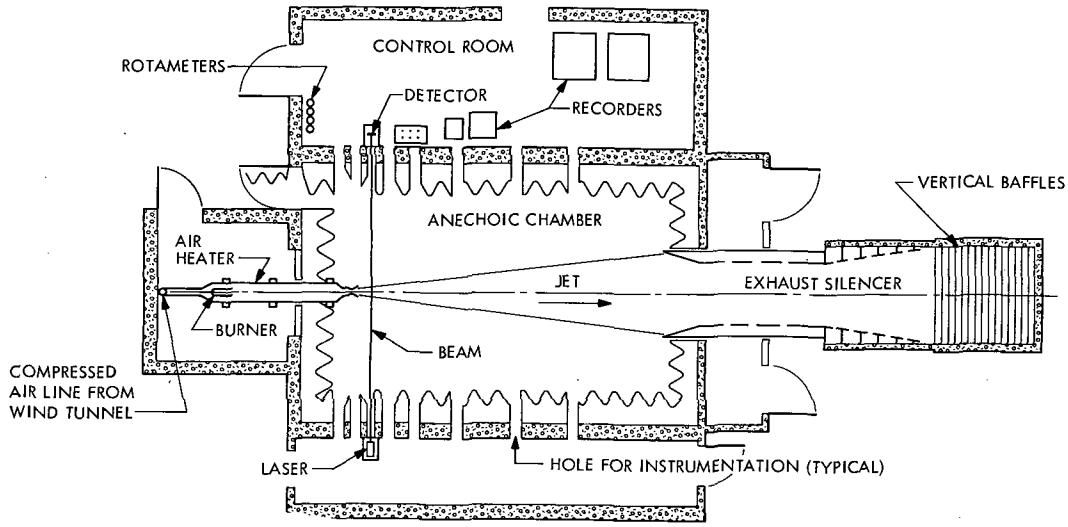

Fig. 1. Jet noise facility

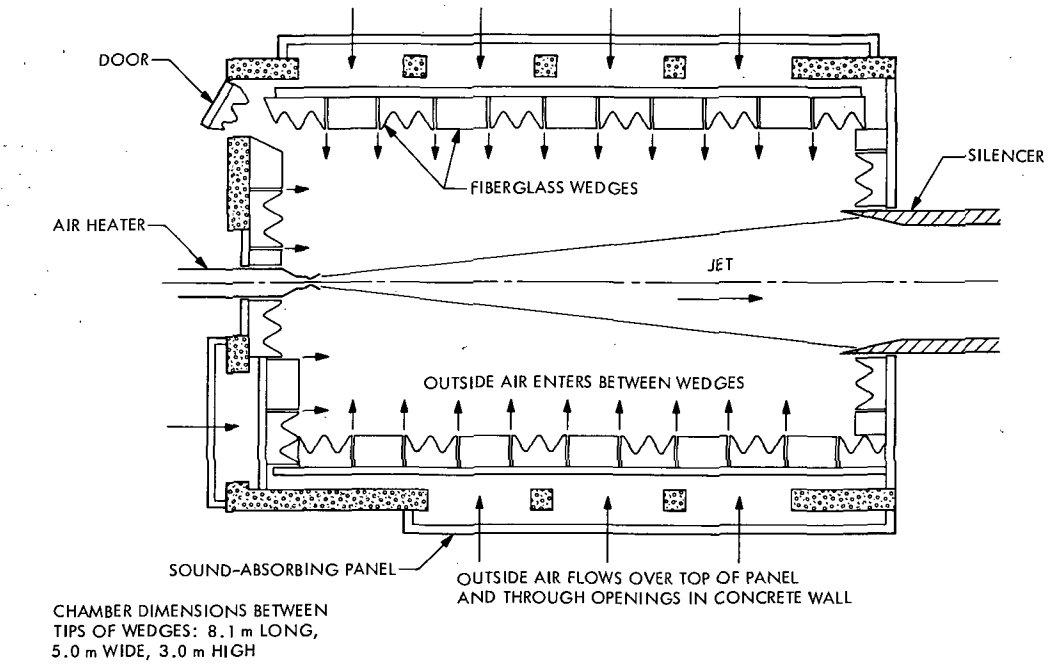

Fig. 2. Anechoic chamber—plan view

Fig. 3. Sound-absorbing panel with outside air intake

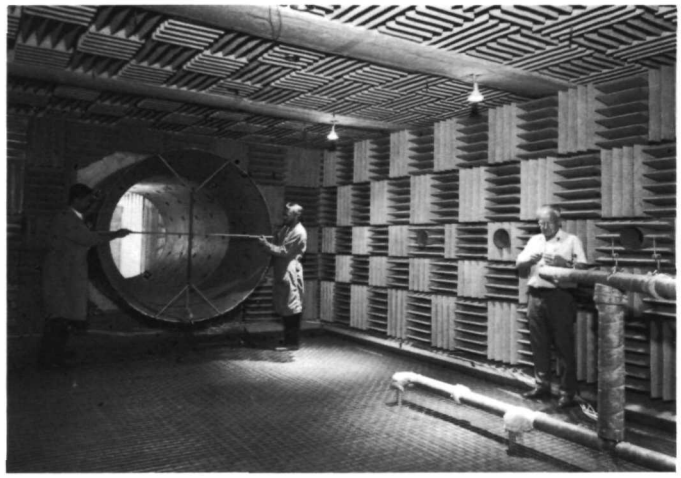

Fig. 4. Photograph of anechoic chamber showing inlet of exhaust silencer

at this and at lower frequencies contribute only a small fraction to the total noise radiated from jets and consequently do not need to be taken into account unless this part of the spectrum is of particular interest. Information at even lower frequencies can be obtained, however, either if the noise-sensing elements (microphones) are confined to locations that are not too close to the exhaust silencer or to the wedges, or if the data are corrected for reflections. Calibration of the chamber is discussed later in this section.

The wedge blocks (Figs. 4 and 5) are mounted on horizontal tracks and are spaced approximately 2 cm apart to permit outside air to enter the chamber. These blocks can easily be moved along the tracks in order to adjust spacing. They can also be easily removed from the tracks, a desirable feature since it permits experiments to be observed from outside the room through windows when the wedge blocks covering them are taken off the tracks. The fiberglass is covered with No. 2 mesh hardware cloth to prevent erosion or tearing by the air flow drawn in from the outside.

The ceiling and the two walls parallel to the axis of the jet contain round holes, about 14 and 23 cm in diameter, respectively, whose centers are in line with the jet axis. These holes, which can be seen in Figs. 4 and 5, extend through the wedge blocks and may be used for optical measurements, such as the use of crossed laser beams to evaluate fluctuating quantities. There is also a rectangular opening about 1 m square in each side wall for greater viewing area. All of these openings, both in the walls and in the ceiling, are covered with

Fig. 5. Photograph of anechoic chamber showing nozzle and support for microphones

metal plates attached on the exterior surfaces when the holes are not being used for instrumentation purposes. Quartz or lucite windows are placed over the openings when optical instrumentation is employed.

The air heater, with an attached nozzle, extends through the wall at one end of the chamber (Fig. 5), and the exhaust silencer captures the jet at the opposite end (Fig. 4). Access to the room is provided by means of a refrigerator-type door, which is also lined on the inside surface with wedge blocks. The spring-loaded wire-cable

floor woven with a 5 × 5 cm mesh, also visible in Figs. 4 and 5, which provides the support for personnel walking inside the chamber, is located 16 cm above the tips of of the wedge blocks that are laid directly on the concrete floor. Numerous stanchion supports are provided, and holes were cut through the wedge blocks so that pipes can easily be attached to the supports, which are mounted on the floor. The stanchions are used to support microphones, as shown in Fig. 5, aerodynamic instrumentation such as pressure and temperature probes, and other instrumentation.

Calibration of the anechoic chamber in terms of sound absorption was accomplished by measuring the sound pressure levels (intensities) at numerous locations, with noise being emitted from a single noise source at a fixed location. In a strictly anechoic chamber, there would be no reflections and the intensity of sound would decrease as the square of the distance from the source (6 dB for every doubling of the distance from the source). However, because of the presence of a silencer that projects a short distance into the room and the lower cutoff frequency of the wedge blocks, reflections do occur to some extent, more at some frequencies than at others. Reflections from the wire-cable floor are negligible at distances of 10 cm or more above the wires.

The noise source used for the calibration was a 15-cm speaker driven by a random noise generator and positioned in the room as shown in Fig. 6, which also shows contours of the overall sound pressure level. The overall intensity, as well as the intensity in octave bands, of the sound emitted was measured with a B&K portable sound level meter. During the measurements, the diaphragm of the speaker was always positioned to be perpendicular to the lines along which measurements were being made (A through I, as indicated in Fig. 6). This eliminated any effects of directionality that the noise emitted by the speaker could have on the sound pressure level (SPL) contours. The lines along which measurements were made were all located in the horizontal plane, passing through the center of the chamber. Data were recorded at distances of 120, 160, 200, 240, 320, 440, 560, and 680 cm from the speaker. From these measurements, contours of equal sound pressure in decibels were constructed for each octave band. The results are shown in Figs. 7 through 17. In a chamber that is perfectly anechoic, these contours would be circles centered at the speaker; thus, departures from circles indicate that reflections exist. Also, in an ideal anechoic chamber, the SPL in any octave band can be evaluated by the equation

$$p(r) = p(r_0) - 20 \log_{10}\left[\frac{r}{r_0}\right] \tag{1}$$

where r and r_0 are the distances from the source.* If the measured SPL is denoted as $p'(r)$, then a measure of the quality of the chamber is indicated by the departure from the inverse square relationship of Eq. (1), which will be denoted as ϵ. Thus,

$$\epsilon = p'(r) - p(r) \tag{2}$$

Substituting Eq. (1) into Eq. (2) gives

$$\epsilon = p'(r) - \left\{p(r_0) - 20 \log_{10}\left[\frac{r}{r_0}\right]\right\} \tag{3}$$

If it is assumed that $p'(r_0) = p(r_0)$ at r_0 close to the source, the values of ϵ can be obtained from the measurements. These values of ϵ are given in Tables 1 through 9.

It is seen from the tables that ϵ is comparatively large ($|\epsilon| > 2$) and negative in the 32-kHz band. The reason for this is attenuation of sound in air, which can be about 1 dB/m at 30 kHz; thus, measured values are less than the inverse square relationship, as indicated by the negative sign, and increase negatively with distance. At intermediate frequencies, the departure from an inverse square distribution is smaller. Then, at the low end of the spectrum (e.g., 31 and 62 Hz and, to a smaller extent, in the 125-Hz band), the value of ϵ is again comparatively large. In this range, the fiberglass wedges do not absorb sound as well because of their low-frequency design limitation, and reflections occur which can make the values of ϵ either positive or negative. There is a comparatively large region in the anechoic chamber that extends downstream from the nozzle (or speaker) where ϵ is low (0 to 1 dB), and this is where most of the jet noise measurements are made. Along the direction of maximum emission from the jet (i.e., along lines B, C, G, and H) ϵ is small over a large part of the distance from the speaker.

The value of ϵ is larger along lines B and C because the booms which support the microphones for the jet noise experiments were present during these tests, whereas there were no such supports on the other side of the chamber. These booms are wrapped with fiberglass that is 5 cm thick; nevertheless, they do reflect somewhat at the lower frequencies. Regions in which ϵ varies between various limits are shown in Fig. 18.

*Parentheses denote "function of" in all of the equations.

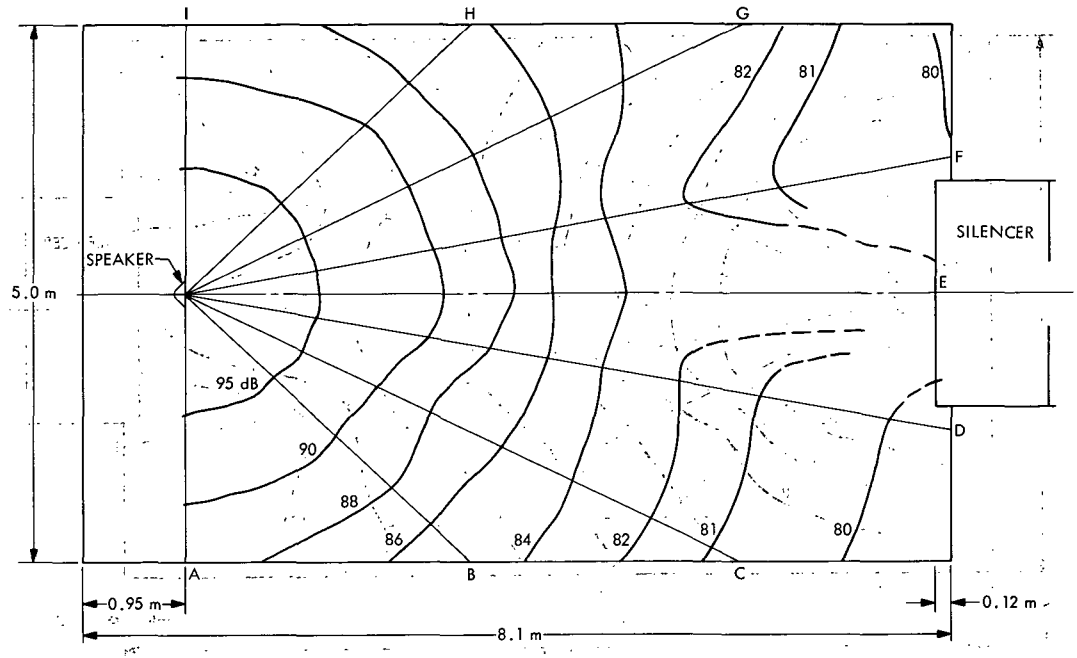

Fig. 6. Contours of overall sound pressure level radiated from a single speaker

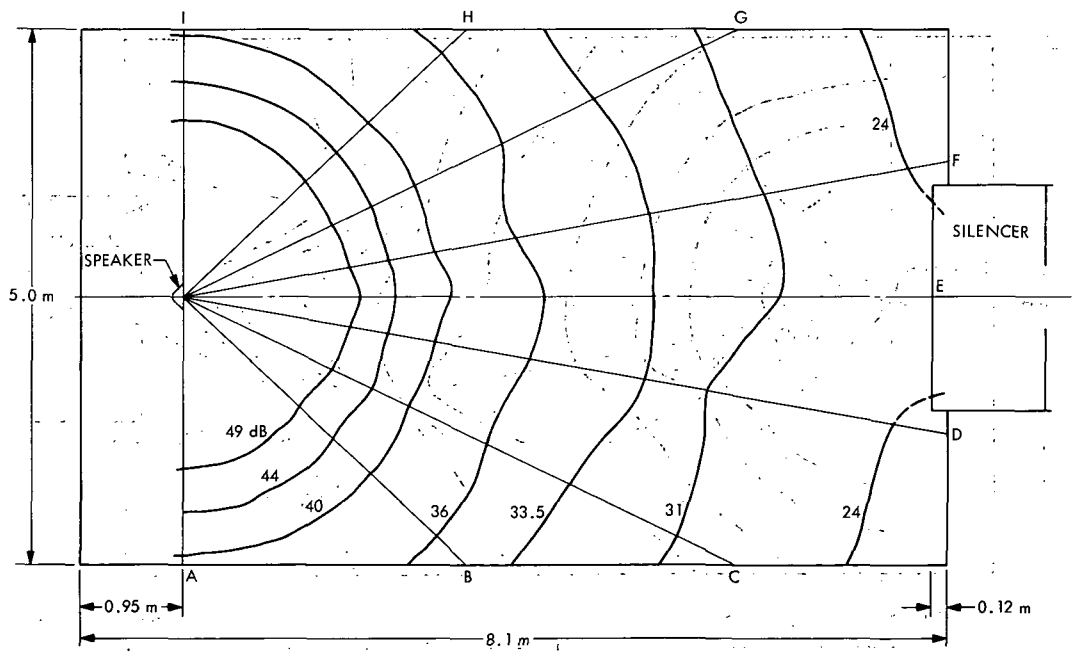

Fig. 7. Contours of sound pressure level in the 31.5-kHz octave band

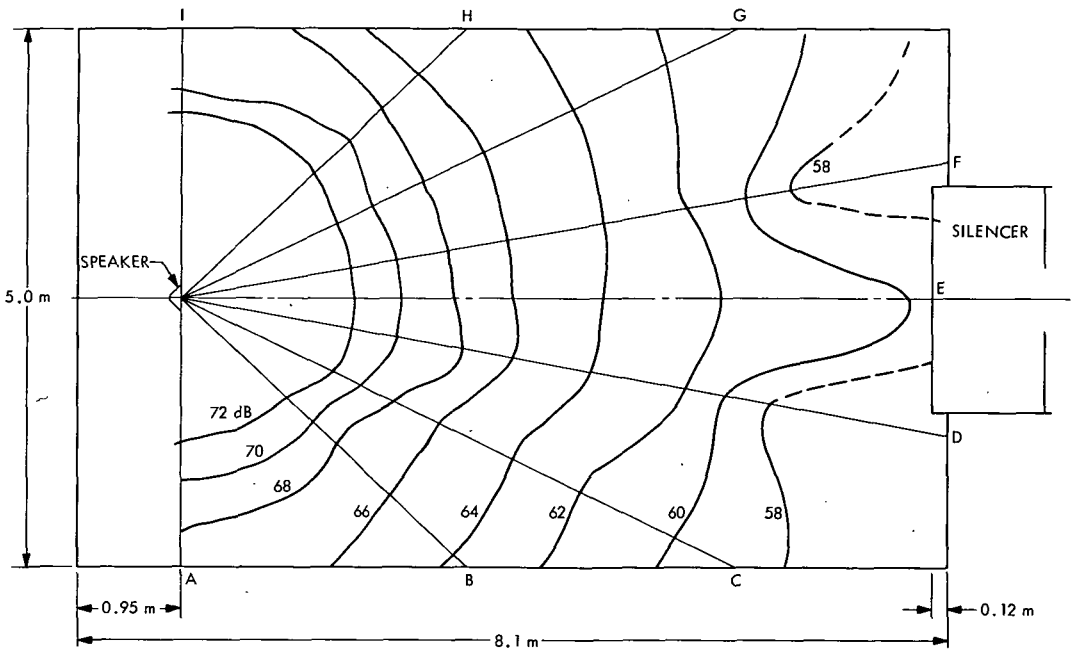

Fig. 8. Contours of sound pressure level in the 16-kHz octave band

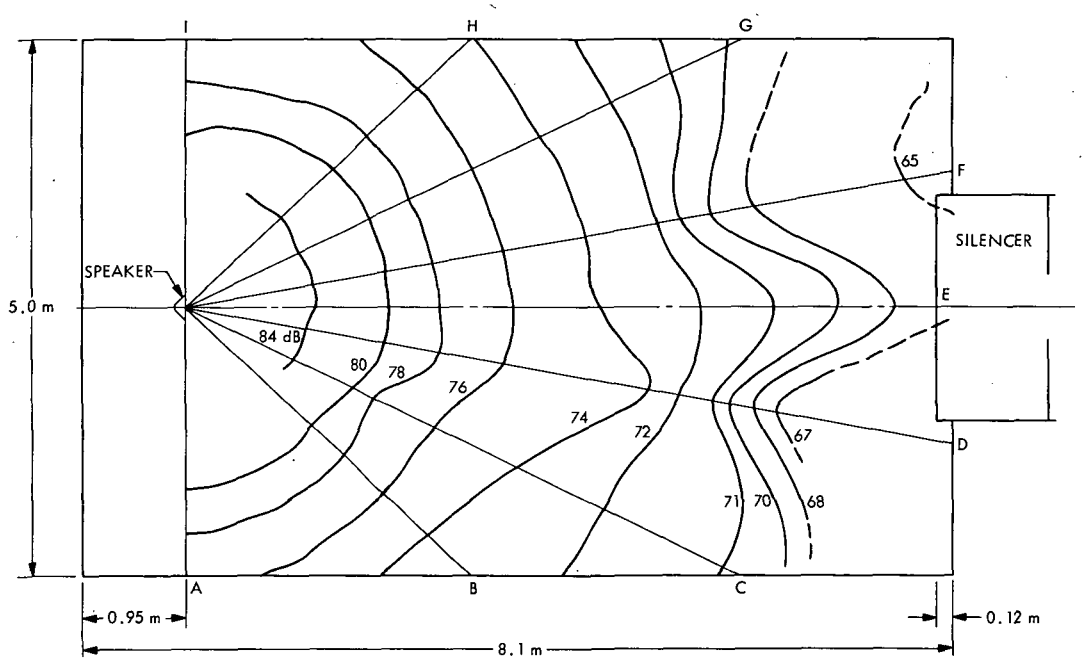

Fig. 9. Contours of sound pressure level in the 8-kHz octave band

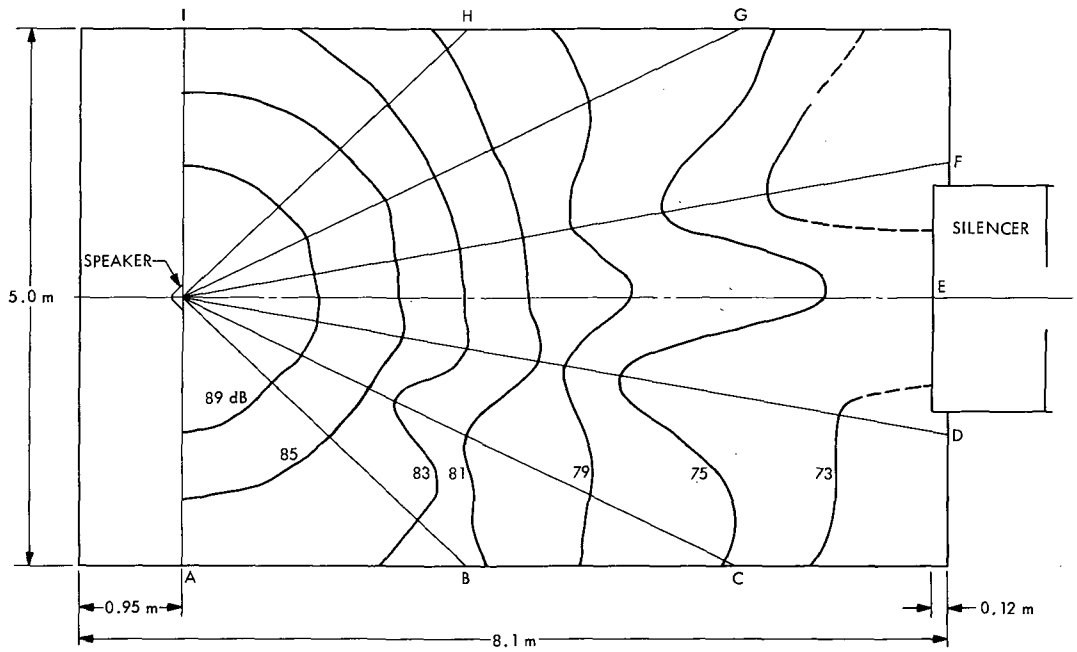

Fig. 10. Contours of sound pressure level in the 4-kHz octave band

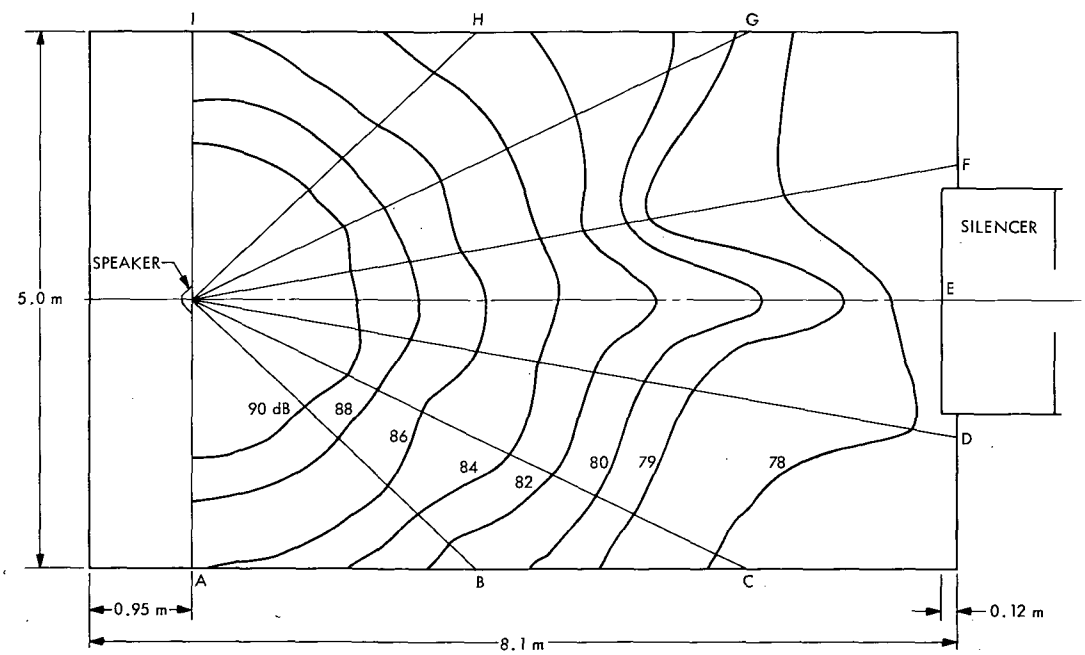

Fig. 11. Contours of sound pressure level in the 2-kHz octave band

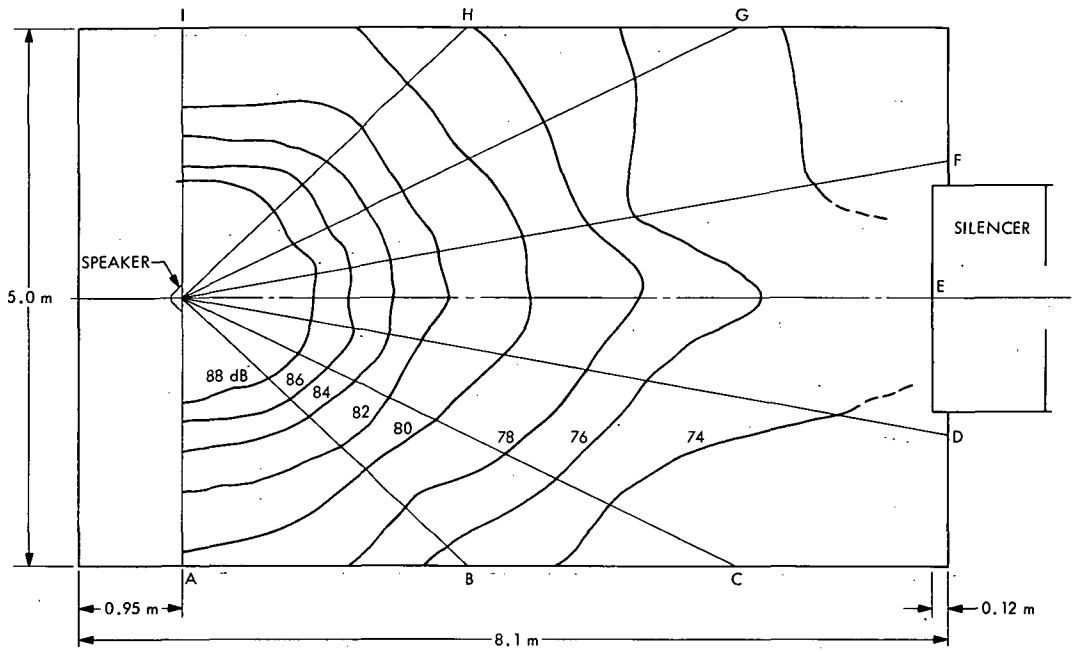

Fig. 12. Contours of sound pressure level in the 1-kHz octave band

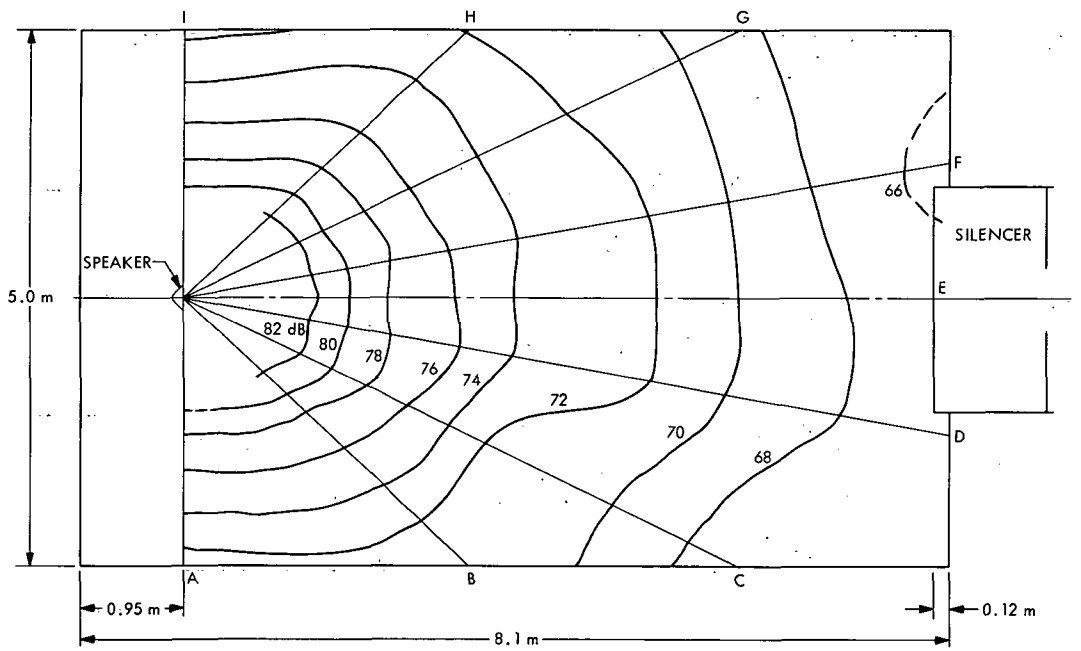

Fig. 13. Contours of sound pressure level in the 500-Hz octave band

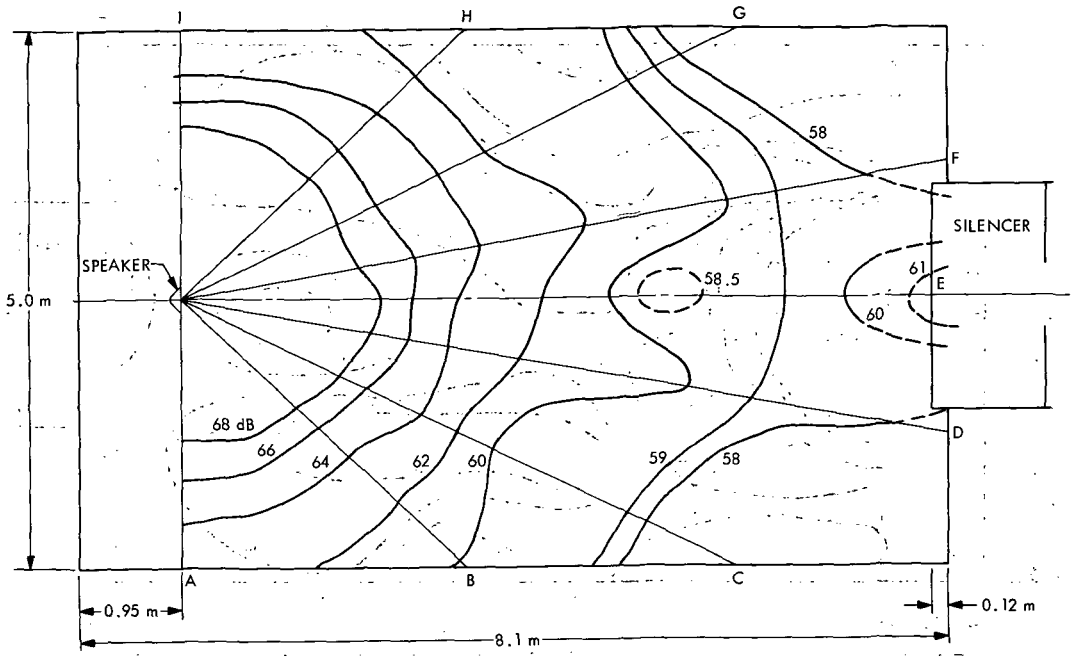

Fig. 14. Contours of sound pressure level in the 250-Hz octave band

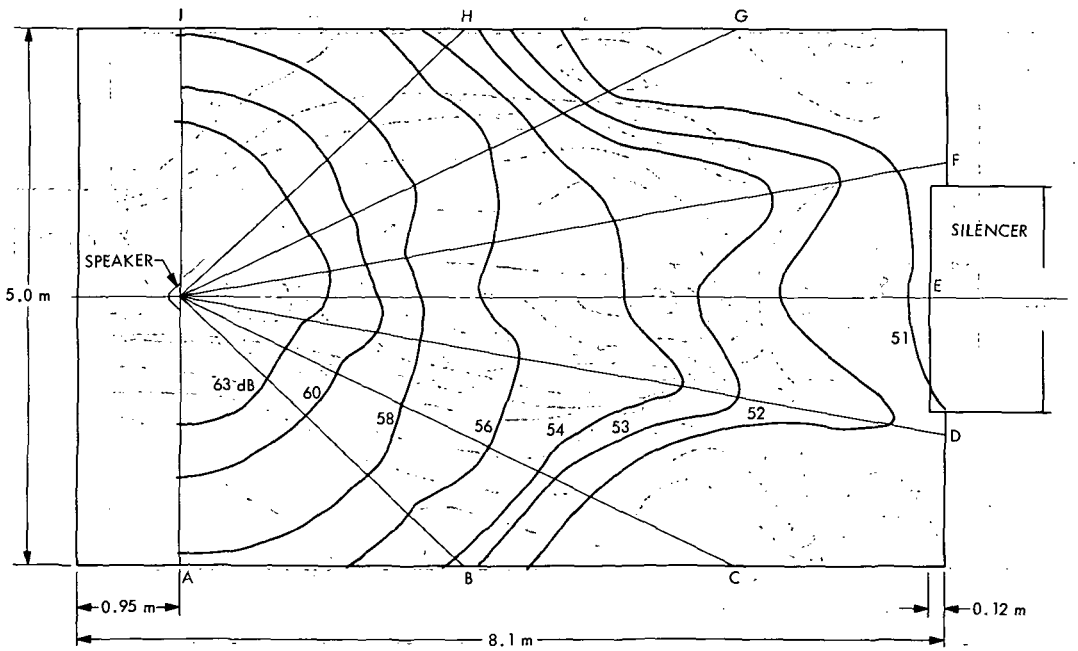

Fig. 15. Contours of sound pressure level in the 125-Hz octave band

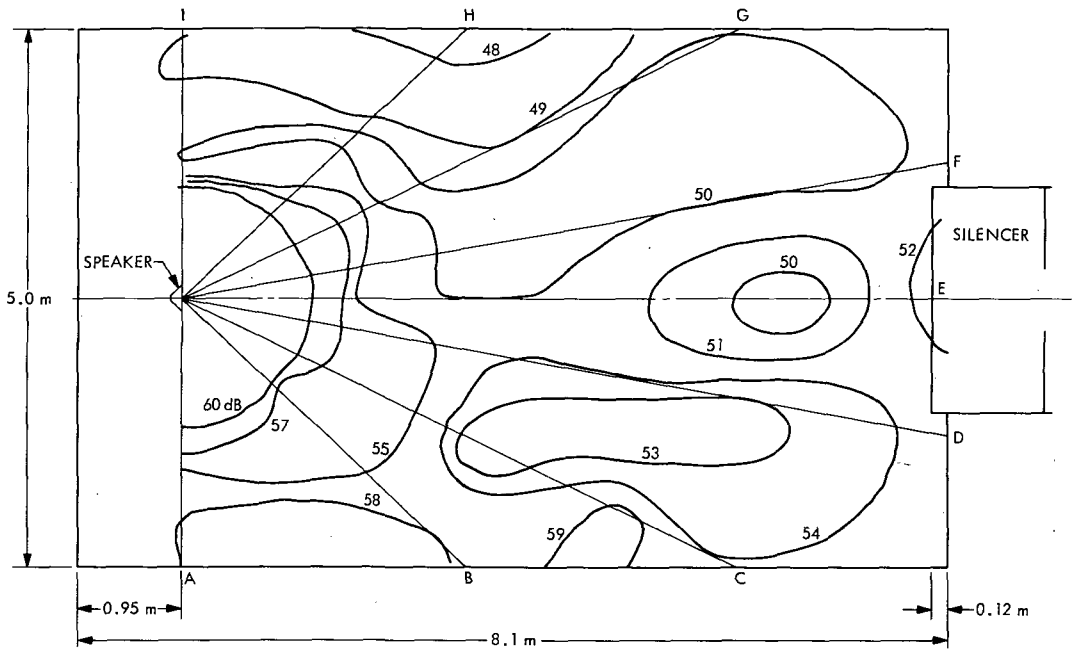

Fig. 16. Contours of sound pressure level in the 62.5-Hz octave band

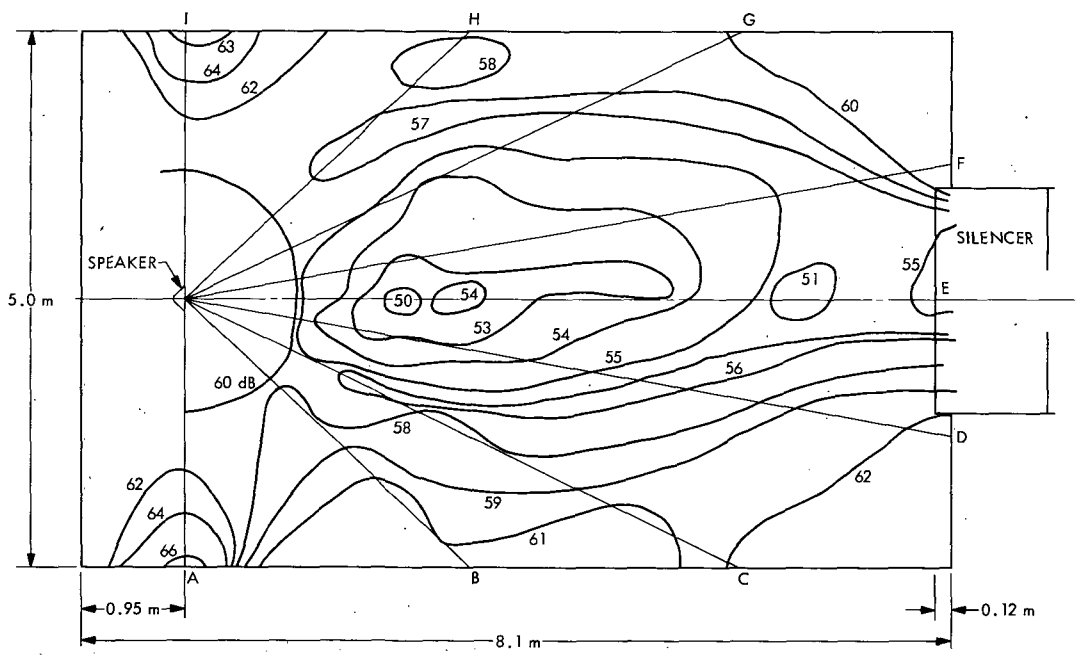

Fig. 17. Contours of sound pressure level in the 31.2-Hz octave band

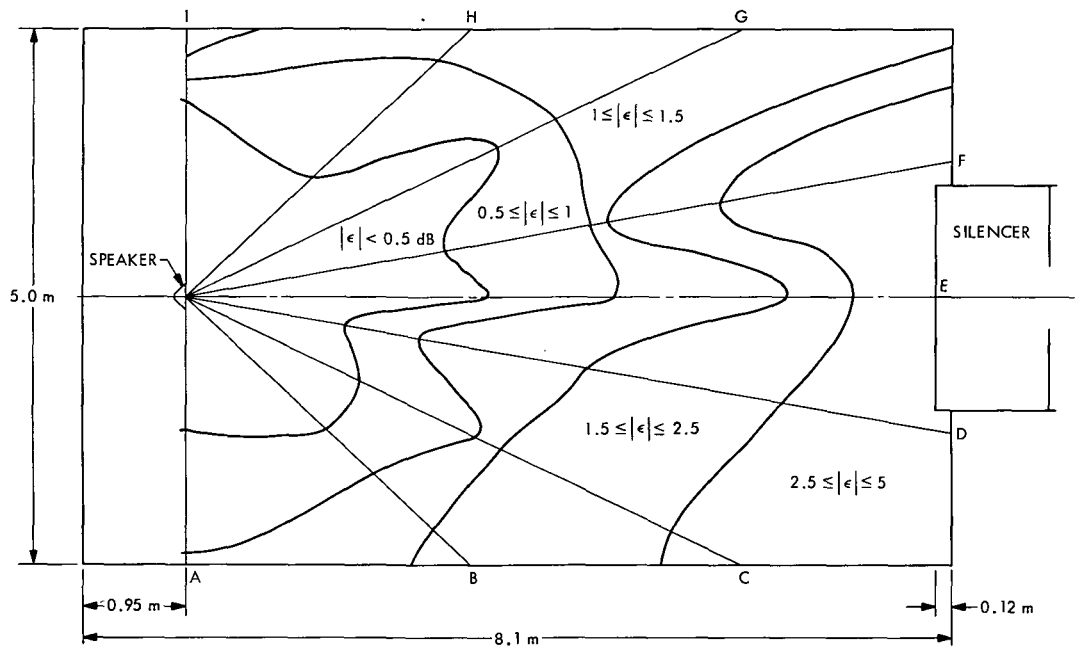

Fig. 18. Ranges of ϵ in various regions of the anechoic chamber

Table 1. Differences in sound pressure level between an inverse square relationship and measured values along line A of Figs. 6 through 17; $\epsilon = p' - p$ (dB)

Frequency, Hz	Distance from speaker, m		
	1.6	2.0	2.4
Unfiltered	0	0	0.1
32K	−1.8	−1.9	2.8
16K	0	0.4	−0.7
8K	0	0	−0.2
4K	0.2	0.8	0.7
2K	0	0.2	0.5
1K	0.6	0.4	0.6
500	0.2	0.1	−1.1
250	0	−0.1	−0.8
125	0	−1.1	0
63	−2.5	2.4	4.0
31.5	1.5	5.4	9.0

Table 2. Differences in sound pressure level between an inverse square relationship and measured values along line B of Figs. 6 through 17; $\epsilon = p' - p$ (dB)

Frequency, Hz	Distance from speaker, m			
	1.6	2.0	2.4	3.2
Unfiltered	−0.2	−0.1	0.5	0.2
32K	−1.5	−2.1	−1.8	−2.3
16K	−0.2	−0.8	0.1	0
8K	−0.1	−0.2	−0.3	−0.5
4K	0	−0.4	0.3	1.8
2K	0.2	0.6	1.2	−0.3
1K	−0.3	−0.4	−1.1	−1.8
500	−0.7	−0.3	−0.3	−0.9
250	0	−0.6	−0.5	−0.3
125	0	0.9	1.5	1.1
63	0.5	1.4	4.0	9.5
31.5	2.5	5.3	9.0	11.5

Table 3. Differences in sound pressure level between an inverse square relationship and measured values along line C of Figs. 6 through 17; $\epsilon = p' - p$ (dB)

Frequency, Hz	Distance from speaker, m					
	1.6	2.0	2.4	3.2	4.4	5.6
Unfiltered	0	−0.8	−0.7	−0.3	−1.0	−1.0
32K	−2.2	−3.4	−3.5	−4.2	−3.7	−4.1
16K	0	−1.1	−0.8	−1.3	−1.7	−1.6
8K	0.2	−0.9	−0.8	−0.1	0	1.3
4K	0.3	−0.6	−0.5	−0.7	0.9	−0.8
2K	0.2	−0.2	−0.5	0.5	−1.8	−1.1
1K	−0.3	−0.9	−1.1	−0.8	−2.5	−0.7
500	0	−0.6	−0.5	−1.8	−0.7	−1.6
250	0.4	−0.9	−0.3	−2.3	1.5	−3.4
125	0	0.9	1.0	2.0	0.3	−1.6
63	−1.5	−1.6	1.0	1.5	6.3	7.4
31.5	3.5	5.4	9.0	11.5	17.3	20.4

Table 4. Differences in sound pressure level between an inverse square relationship and measured values along line D of Figs. 6 through 17; $\epsilon = p' - p$ (dB)

Frequency, Hz	Distance from speaker, m						
	1.6	2.0	2.4	3.2	4.4	5.6	6.8
Unfiltered	0.1	0.2	0.3	0.5	−1.7	−1.1	−0.3
32K	−1.8	−2.2	−2.8	−3.3	−2.5	−4.4	−5.7
16K	0.6	0.7	1.0	0.3	1.3	−2.8	−3.6
8K	0.2	0.4	0.4	0.2	−1.3	−3.4	−2.9
4K	0.2	0.3	0.5	0.7	−3.3	−2.6	−0.5
2K	0.1	0	0.1	0.6	−2.1	−1.0	0.6
1K	0.5	0.2	0	0.3	−0.7	0.4	0.1
500	0.5	0.7	1.3	0.5	1.8	0.6	0.9
250	0	−0.1	−1.0	−1.0	0.5	0.4	1.6
125	0	0.4	0.5	1.5	2.8	2.9	4.1
63	−2.0	1.4	1.0	2.5	5.3	6.4	9.1
31.5	1.5	3.4	5.0	8.5	13.3	18.4	23.1

Table 5. Differences in sound pressure level between an inverse square relationship and measured values along line E of Figs. 6 through 17; $\epsilon = p' - p$ (dB)

Frequency, Hz	Distance from speaker, m						
	1.6	2.0	2.4	3.2	4.4	5.6	6.8
Unfiltered	0.5	0.4	0.7	0.7	0.5	1.1	2.3
32K	−3.7	−7.1	−8.8	−10.0	−11.0	−12.1	−10.4
16K	0.2	0.3	0.2	−0.1	0	0.1	0.8
8K	0	−0.4	−0.2	−0.2	0	0.2	−0.2
4K	0	0.1	0.4	0.2	0.5	−0.1	2.6
2K	0.3	0.2	0.5	0.5	0.6	1.6	1.1
1K	0	0.1	0.3	0.5	1.1	1.7	3.1
500	−0.5	−0.4	−0.2	−0.5	1.0	−0.2	0.3
250	−0.5	0.4	−0.5	0	−1.2	1.4	5.1
125	−1.2	−1.3	−1.7	−1.2	0.1	0.7	1.3
63	−2.5	−3.6	−4.0	−1.5	2.3	2.4	7.1
31.5	−1.5	−2.6	3.0	4.5	7.3	7.4	13.1

Table 6. Differences in sound pressure level between an inverse square relationship and measured values along line F of Figs. 6 through 17; $\epsilon = p' - p$ (dB)

Frequency, Hz	Distance from speaker, m						
	1.6	2.0	2.4	3.2	4.4	5.6	6.8
Unfiltered	0.5	0.1	0.4	0.5	−1.7	−0.9	0.3
32K	−3.9	−7.1	−8.7	−10.7	−9.9	−11.3	−12.1
16K	0	0.1	0.2	−0.7	0.6	2.8	−3.6
8K	0	−0.3	−0.2	−0.3	−0.4	−4.1	−3.9
4K	0.3	0.2	0.5	0.3	−2.7	−3.0	−1.4
2K	0.5	0.1	0.2	0.5	−2.7	−1.1	−0.7
1K	0	0	−0.2	0.3	−1.3	−0.3	−0.4
500	−0.2	0.2	0.3	0.2	1.3	0.1	−0.9
250	0.2	−0.1	0.5	0	1.8	1.4	1.6
125	−2.0	−2.1	−2.0	−1.0	−0.2	1.4	1.1
63	−2.0	−4.6	−4.0	−1.5	1.3	1.4	5.1
31.5	−1.5	−0.1	3.5	4.5	7.8	10.9	17.6

Table 7. Differences in sound pressure level between an inverse square relationship and measured values along line G of Figs. 6 through 17; $\epsilon = p' - p$ (dB)

Frequency, Hz	Distance from speaker, m					
	1.6	2.0	2.4	3.2	4.4	5.6
Unfiltered	0.3	0.2	0.3	0.6	0.3	0.7
32K	−4.1	−7.2	−9.3	−10.5	−10.3	−10.9
16K	0.3	0.2	0.1	0.1	0.1	0.2
8K	0.1	−0.1	−0.2	0	−0.4	−0.3
4K	0.4	0.4	0.3	0.2	0.5	−0.1
2K	0.1	0.4	0.3	0.5	0.1	0.2
1K	0.2	−0.3	0	0.2	0.1	0.6
500	−0.7	−0.1	−0.3	−0.2	0.5	0.4
250	−0.2	−0.3	0.3	−0.5	1.4	−1.0
125	−0.5	−1.1	0	0.5	−1.7	−2.1
63	−3.0	−5.1	−3.5	−2.0	1.8	3.9
31.5	−1.5	1.4	2.0	5.5	10.3	15.4

Table 8. Differences in sound pressure level between an inverse square relationship and measured values along line H of Figs. 6 through 17; $\epsilon = p' - p$ (dB)

Frequency, Hz	Distance from speaker, m			
	1.6	2.0	2.4	3.2
Unfiltered	−0.2	0.2	0.1	0
32K	−4.5	−7.1	−8.7	−10.7
16K	0.5	0.4	0.2	−1.0
8K	0	−0.4	−0.3	−0.5
4K	0.3	0.4	0.5	0.8
2K	−0.2	−0.1	−0.2	0.2
1K	−0.2	−0.3	−0.2	−0.5
500	0	0	0.3	0.3
250	−0.5	−0.6	−0.7	−1.2
125	−0.5	−0.6	0	0
63	−3.5	−4.1	−3.5	−2.0
31.5	0.5	2.4	4.0	7.5

Table 9. Differences in sound pressure level between an inverse square relationship and measured values along line I of Figs. 6 through 17; $\epsilon = p' - p$ (dB)

Frequency, Hz	Distance from speaker, m		
	1.6	2.0	2.4
Unfiltered	0	0.2	0.2
32K	−1.2	−1.6	−2.0
16K	0.2	0.6	0
8K	0	0.5	0.3
4K	0.3	0.7	0.1
2K	0.2	0.3	0.2
1K	−0.7	−0.8	−0.3
500	0	−0.1	0
250	0.2	−1.1	−2.5
125	0.5	0.9	1.0
63	0.5	3.4	5.0
31.5	4.5	8.4	9.0

The shape of the spectrum emitted by the speaker in terms of sound pressure level is shown in Fig. 19, indicating that the response of the speaker was not uniform. For the experimental determination of sound pressure levels, any smooth spectral shape would have been satisfactory.

When the inlet of the silencer projects into the anechoic chamber, the reflections in some regions of the chamber are larger, as expected. For the overall SPL, this is apparent when the 84-dB contour of Fig. 20 (with the silencer projected into the room) is compared with the corresponding contour line of Fig. 6, where the silencer is in the retracted position. In the regions where measurements of jet noise are generally made (closer to the speaker), there is very little difference between the two cases.

If the anechoic chamber were to be used for measurements of noise from sources which are not associated with a large flow of gas, the entrance of the silencer could be covered with fiberglass wedges installed as on the walls. In this case, the quality of the chamber would improve in that there would be no reflections from the silencer and measurements could then be made anywhere inside the room with very little error (0 to 1 dB).

III. Exhaust Silencer

The purpose of the exhaust silencer is to attenuate the noise of the jet to an acceptable level for safety requirements after the flow has passed through the anechoic chamber and extended outside the building. The silencer, as shown in Figs. 21 and 22, consists of a circular inlet, a diffuser which is a transition from the circular inlet to a square duct, a right-angle bend, and a vertical baffle section. The inlet of the silencer is 2.06 m in diameter.

The horizontal part of the silencer can be moved along its axis by removing or adding square sections, so that the inlet can be positioned properly inside the anechoic chamber to just capture the jet as it leaves the chamber. The inlet can be extended as much as 1.5 m into the chamber. The diameter of the jet approaching the silencer will vary with flow conditions.

The inlet section contains cavity resonators (Fig. 23) which attenuate the low-frequency noise in the range between 80 and 200 Hz. The vertical section located farther downstream which contains baffles attenuates the higher frequencies. The inlet and diffuser sections (1 and 2 in Fig. 21) are made of steel, whereas the elbow is concrete. The sound-absorbing baffles are standard, commercially available, 10.2-cm (4-in.) thick, perforated panels.

The attenuation of noise within the silencer, obtained by measurements made using a speaker near the inlet as a noise source, is shown in Fig. 24. It is evident that the attenuation at low frequencies is the largest. The irregularity at 8 kHz is caused by reflections within the silencer, and the relatively large attenuation of 10 dB at 32 kHz is primarily due to absorption in the air between measuring stations A and B.

To evaluate the effectiveness of the silencer in terms of noise absorption between the jet and the outside environment, measurements of the noise level were made at a distance of 5 m from the vertical stack, with a jet flowing through the silencer. The jet Mach number at the nozzle was about 2, and the stagnation temperature was 1090 K (1500°F). Figure 25 shows these outside measured SPL values (squares), as well as some that were obtained inside the anechoic chamber 2 m from the nozzle exit plane (circles) at the same jet flow conditions. The inside measurements were "corrected" to the silencer inlet location by application of the inverse square relationship to the data obtained at the measuring station. This was done in order to better evaluate the attenuation caused by the silencer itself. These "corrected" computed values are shown as triangles in Fig. 25. Also, since there was ambient noise outside the silencer without the jet operating, this ambient contribution was subtracted from those outside measurements that were obtained during jet flow conditions. The difference between these measurements represents the contribution of the jet only, and the data points are shown as diamond-shaped symbols in Fig. 25. The actual measured values of the two outside conditions with and without jet flow are shown in Fig. 26. It is evident that the attenuation of the jet noise by the silencer (the difference between the triangular and the diamond shaped symbols of Fig. 25) ranged from about 35 to 55 dB over the frequency band range, as indicated. Thus, the maximum SPL value of about 108 dB near the silencer inlet was reduced to a maximum of 60 dB outside.

In Fig. 26, a predicted curve (which formed the basis for the design of the silencer) is shown in terms of the sound pressure level at the inlet of the silencer over the indicated frequency band. Also shown are the predicted reduced noise levels that result from use of the baffles only, as well as the combined effect of the baffles

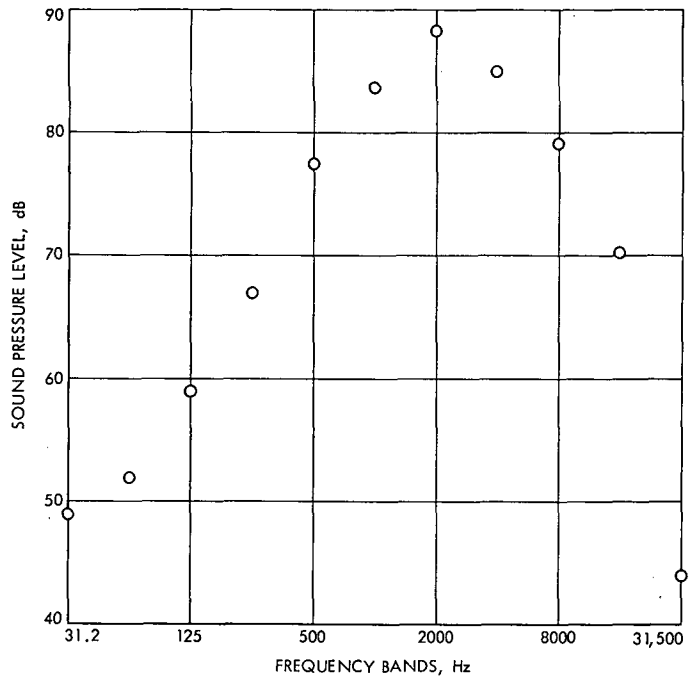

Fig. 19. Spectral distribution of noise used for calibrating the anechoic chamber

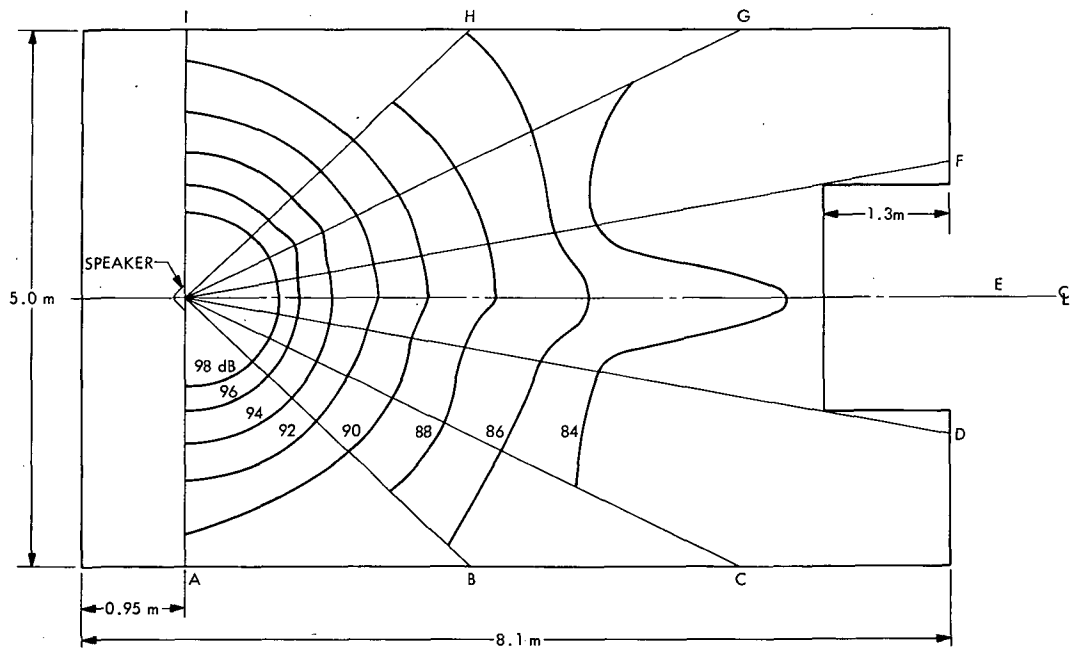

Fig. 20. Contours of overall sound pressure level of noise radiated from a single speaker with exhaust silencer extended into anechoic chamber

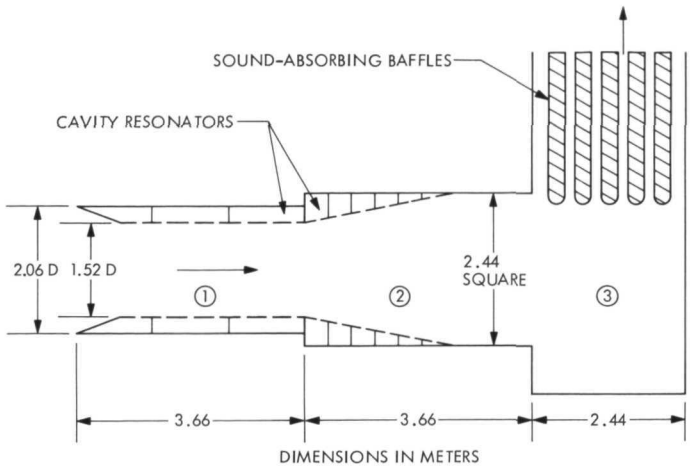

Fig. 21. Exhaust silencer

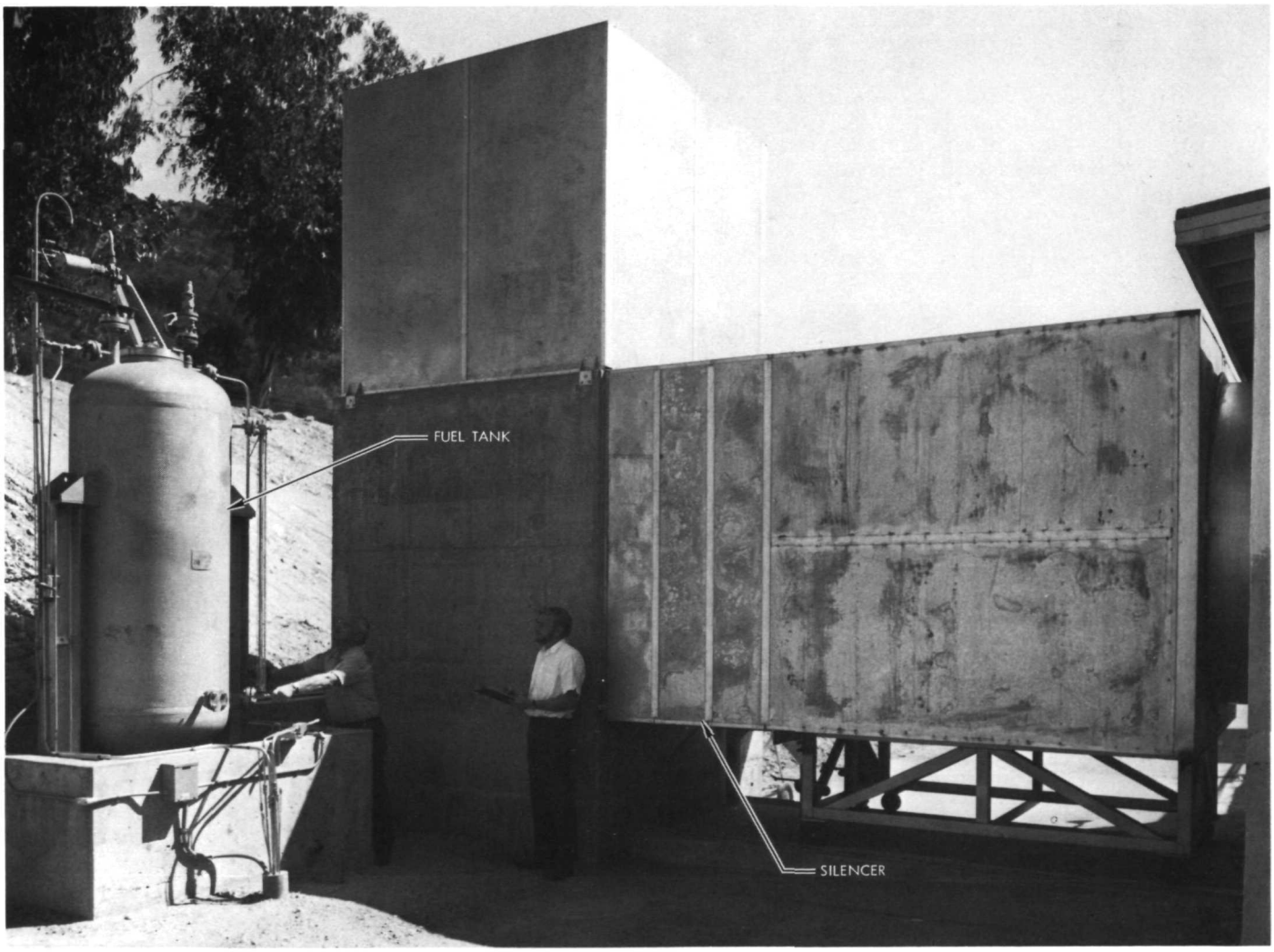

Fig. 22. Photograph of exhaust silencer and fuel tank

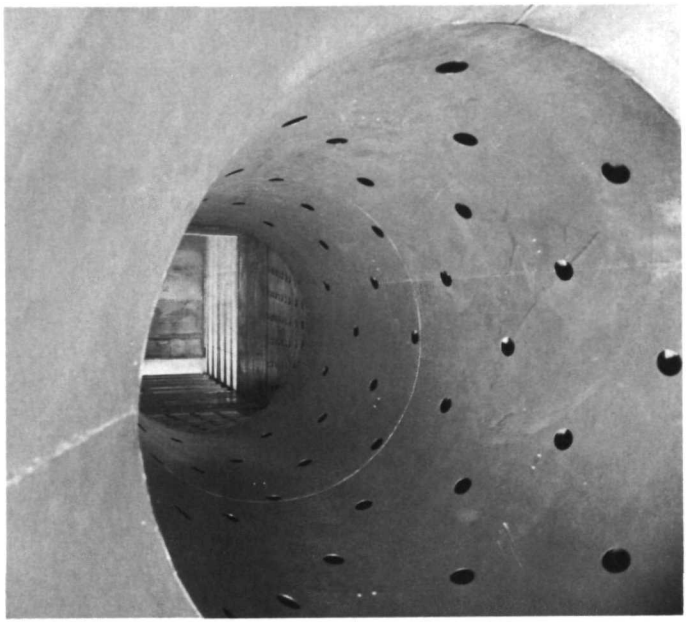

Fig. 23. Inlet section of exhaust silencer showing openings to cavity resonators

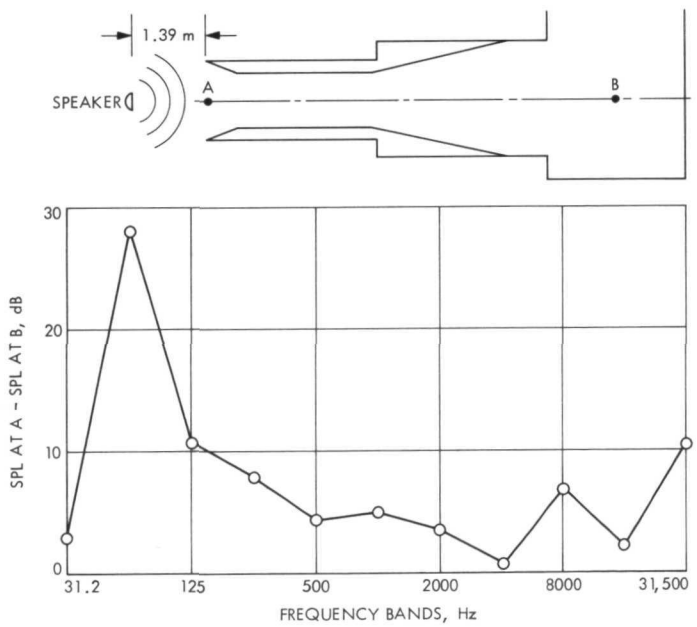

Fig. 24. Noise attenuation within exhaust silencer

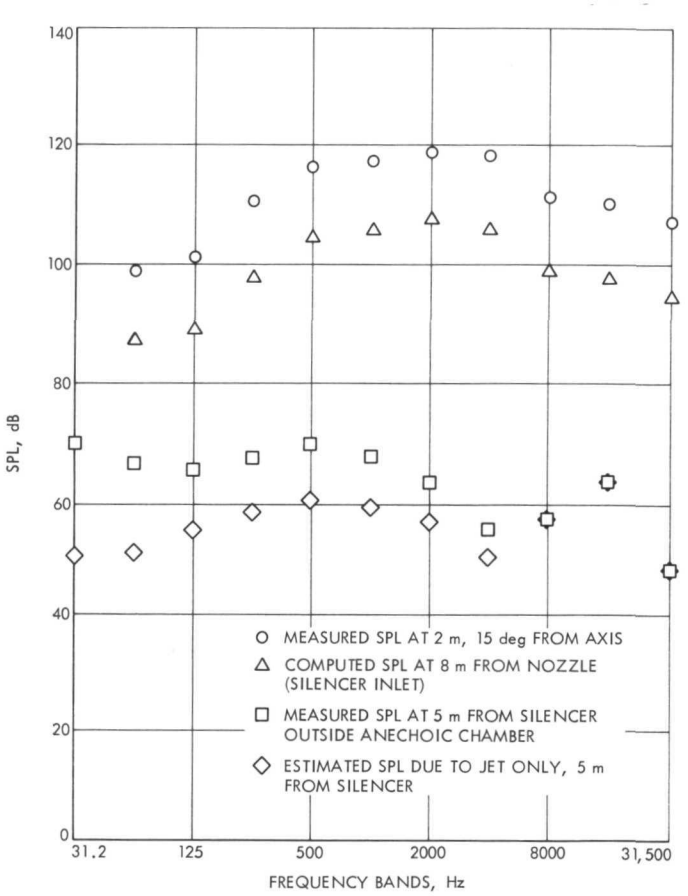

Fig. 25. Measured effectiveness of exhaust silencer

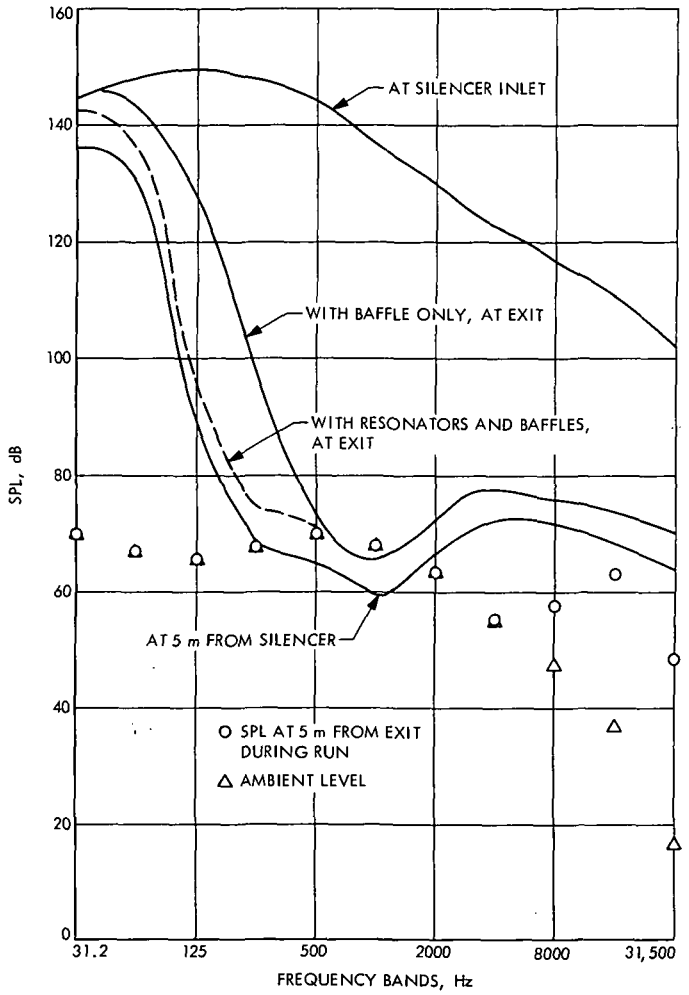

Fig. 26. Design effectiveness of exhaust silencer

and the resonators. In addition, the noise level that was expected at a distance of 5 m from the silencer is indicated. It is evident that the purpose of the resonators was to reduce the noise at the lower frequencies. Although a comparison of the effectiveness of the silencer based on the design value of the high noise intensity level at the inlet has not yet been made, it is evident in Fig. 25 that substantial attenuation occurs over the entire frequency spectrum.

IV. Air Heater

The air heater consists of a burner section, and a mixing and calming section. A flow straightener and an afterburner section with a fuel spray bar and a flame holder can be installed just upstream of the nozzle, as shown in Fig. 27. A photograph of the heater is presented in Fig. 28. A steady flow of compressed air at about room temperature enters the burner section, where approximately 90% of the mass flow rate passes through holes in a turbojet burner can. Here fuel is injected and combustion occurs. This flow then enters a mixing and calming section. The remaining 10% of the entering air flow is bypassed to an annular flow channel located between the wall of the 30.5-cm-diameter duct and a liner. The liner, which is cooled by this gas flow in the annulus, acts as a buffer to prevent the duct wall from overheating. In addition, the duct wall has water coolant tubes placed on the outside surface (Fig. 28). The air that flows through the annulus is heated by the liner and mixes with the primary flow downstream, where the liner is terminated. A honeycomb straightener or screens can be installed near the downstream end of the 30.5-cm-diameter duct where it converges to a 12.7-cm-diameter approach section located just upstream of the nozzle. Provision for afterburning at that location is incorporated into the design. Consequently, the turbulence level of the fluid entering the nozzle can be controlled by the mesh size of the screens and by the use of the afterburner.

The air heater assembly was designed to withstand a working pressure of 35.1 kg/cm^2 (500 psia) at a wall temperature of 810 K (1000°F) on a continuous basis. The maximum allowable stagnation temperature of the gas is about 1640 K (2500°F). The wall temperatures of the larger duct and of the liner are monitored by the use of thermocouples welded to the surfaces. A telescoping duct (Fig. 28) is provided upstream of the burner section to accommodate the longitudinal growth of the air heater duct as the wall temperature increases. An electrical ignition system and a spark plug are provided to ignite the fuel. The burner section also contains a primary and a secondary fuel nozzle at the upstream end of the burner, where combustion is initiated.

V. Fuel System

The fuel system consists of a tank (Fig. 22), associated valves and lines, rotameters for measuring the rate of fuel flow, and a nitrogen pressurization system. The capacity of the tank is 1135 l (300 gal). This fuel supply is sufficient to permit continuous operation for at least 30 min under the most demanding conditions (i.e., maximum allowable gas flow rate and gas temperature). Fuel is forced to flow through the lines and into the burner by the pressure inside the tank which is generated by the nitrogen pressurization system. The purpose of the fuel system is to provide a means of heating the compressed air supplied to the nozzle. Almost any type of air-breathing engine fuel may be used, although

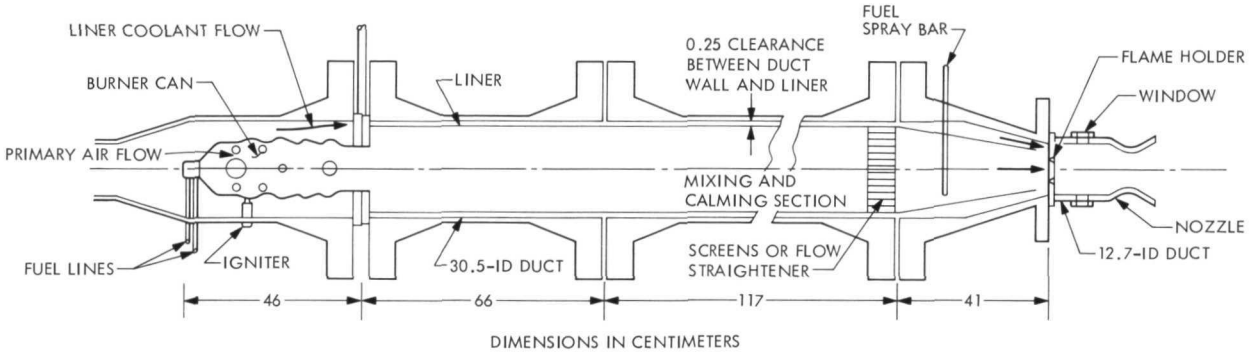

Fig. 27. Air heater

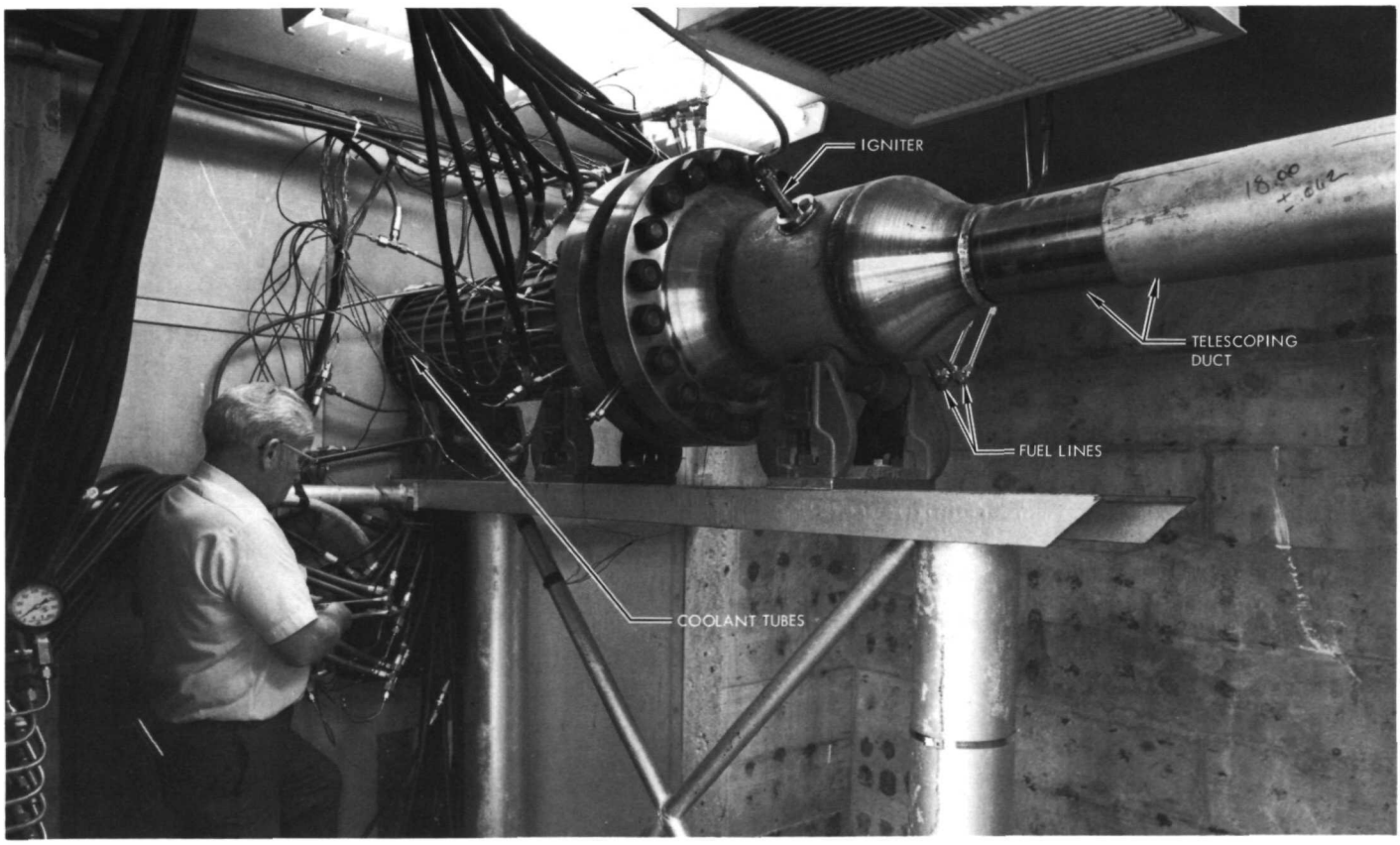

Fig. 28. Photograph of air heater

methanol is commonly employed because carbon residue does not appear on cooled surfaces from the products of combustion of this fuel.

VI. Cooling System

Water obtained from the wind tunnel facility is used to cool the nozzle and portions of the air heater. At a typical water flow rate of about 1.2 kg/s (2.7 lb/s), the supply pressure from the pump is 22.5 kg/cm^2 (320 psi). The water is supplied to a distribution manifold located inside the control room, where rotameters are used to meter the flowrate to each of the coolant passages. After flowing through the apparatus, the water is returned to the wind tunnel supply, where it is cooled by means of cooling towers and then recirculated. Temperature-difference thermocouples are placed in the inlet and outlet lines of the apparatus, so that the temperature differences can be monitored and heat transfer calculations made if desired.

VII. Instrumentation

Provisions have been made for the experimental evaluation of the following quantities associated with the jet as the flow passes through the anechoic chamber: (1) the spatial and the spectral distributions of the intensity of the noise radiated from the jet, (2) the autocorrelation (or spectrum) of the noise sources in their moving frame of reference, (3) the spatial distribution of the density fluctuations within the jet, (4) the moving density autocorrelation and the convection velocity of the eddies, and (5) the mean velocity and temperature distributions of the jet flow. In addition, the thrust on the nozzle and the flow coefficient can be determined; the air and the fuel flowrates are measured; the gas temperature at the nozzle inlet can be evaluated; and the heat-transfer distribution along the nozzle can be obtained by calorimetry if the nozzle contains appropriate coolant passages. Photographs of the flow field can be taken using either a Schlieren or a Shadowgraph system. Explanations of the methods used to determine these quantities are given in the following sections.

A. Noise Distribution

The spectral distribution of the sound pressure levels radiated from a jet flow can be obtained from measurements by using microphones located at various positions surrounding the jet. From contour plots of the sound pressure levels in frequency bands, it is possible to locate approximately the apparent noise sources in each of the corresponding frequency bands.

In a jet flow, however, the noise sources move; consequently, an evaluation of the noise spectrum in the moving reference frame of the sources is useful. Such an evaluation can be accomplished by the use of a cross-correlation method applied to the signals from two spatially separated microphones. This method can best be outlined by first considering noise sources that are stationary. In this case, sound waves produced by different sources reach two spatially separated microphones at different times. The signals from the two microphones are correlated, with a time delay introduced into one of them. As the delay varies, the experimental cross-correlation function separates (along the time-delay axis) the individual autocorrelation functions of the spatially separated sources, provided that the resolution is adequate. When the sources move, sound waves produced by each source reach the pair of microphones with varying delays in time, and the experimental cross-correlation function obtained from the microphone signals is an integral of the autocorrelation function of the moving sources. Thus, the shapes will be distorted and the functions may overlap along the time-delay axis. However, with the use of a suitable statistical model and a trial-and-error method, the autocorrelation function of the moving sources can be obtained. The spectrum of the moving source is then merely the Fourier transform of the autocorrelation function.

B. Density Fluctuations and Eddy Velocity

Instrumentation is provided to evaluate the spatial distribution of the fluctuating density of the eddies in the moving reference frame as well as the convection velocity of these eddies with the use of crossed laser beams. Openings are located in two walls and in the ceiling of the anechoic chamber, as shown in Figs. 1, 4, and 5, so that the measurements can be made at numerous positions along the flow direction of the jet. The flow can also be scanned across the jet. The laser sources are mounted on adjustable supports outside of the room, with the beams directed through the jet perpendicular to the jet axis. Generally, several horizontal beams that are separated vertically are used simultaneously, and these are moved to various axial positions for scanning along the jet. The detectors for the horizontal beams are also located outside of the room, whereas the detector for the vertical beam is mounted on a floor stanchion support. The supports for all detectors are adjustable to facilitate alignment with the beam. The vertical beam is directed perpendicular to the others, and the locations at which they cross (even though they may be displaced horizontally) are the

locations at which the local fluctuating densities are determined.

The principle of the method is as follows. Each beam is arranged as a Schlieren system. The signal detected from each laser is an integration of the gradient of the refractive index across the flow. A cross correlation of the two signals is obtained, and the result isolates the effect of the change in refractive index caused by the eddies (noise sources) which pass through both beams. Typically in the jet noise experiment, the cross-correlation coefficient of the two laser signals is about 0.1. The rms value of the fluctuating density is determined from the constant of proportionality between refractive index and density (Gladstone–Dale constant), the beam lengths, the sensitivities of the photo cells, the intensities of the laser beams, and the gain of the preamplifiers.

It is possible to determine the convection velocity of the eddies by displacing one or more of the beams along the jet axis and delaying the signal from the upstream beam. The velocity is simply the distance between the beams divided by the time delay.

C. Velocity and Temperature Distributions

Both radial and axial distributions of the mean velocity and of the stagnation temperature of the jet flow can be evaluated by means of pitot probes, a static pressure probe, and thermocouple probes. The probes are mounted on a rake (Fig. 4), which can be located at any axial position along the jet and can also be moved perpendicular to the jet axis. The pressures are measured with the use of manometers. When the probe rake is located in a region of comparatively low jet velocities, silicone oil is used as the manometer fluid; in a region of high velocities, mercury is used. The manometers can either be photographed or read visually. Temperatures are recorded by means of a digital recorder.

D. Thrust and Flow Coefficient

The thrust is determined from wall pressures measured along the inner surface of the nozzle. Hence, the atmospheric conditions surrounding the outside of the nozzle are not taken into account. The pressure taps are connected to manometers. Either silicone oil or mercury is used as the fluid, depending upon the magnitude of the pressure difference between adjacent taps.

The flow coefficient C_D is defined as the ratio of the actual mass flowrate to the computed value for one-dimensional isentropic flow. Thus,

$$C_D \equiv \frac{\dot{m}}{\dot{m}_{1\text{-}D}} = \frac{\dot{m}}{p_t A_{th}\left[\frac{\gamma}{RT_t}\left(\frac{2}{\gamma+1}\right)^{(\gamma+1)/(\gamma-1)}\right]^{1/2}} \quad (4)$$

E. Air and Fuel Flowrates

The actual mass flowrate of air, $\dot{m}$, is obtained from pressure and temperature measurements using a venturi located in the compressed-air supply line upstream of the air heater. Fuel flowrates supplied to the burner are determined by rotameters.

F. Gas Temperature

The gas temperature at the nozzle inlet can be determined by two methods: (1) it is measured directly with a thermocouple, or (2) it can be evaluated approximately from the measured flowrates of the fuel and of the air, in conjunction with an energy balance of the air heater. The use of a thermocouple is considered to be the most accurate method. The heating value of the fuel and the efficiency of the burner are needed for calculations based on the air/fuel ratio. Corrections should be made when portions of the air heater are cooled externally.

It can be shown by application of an energy balance to the air heater that the enthalpy of the gas entering the nozzle is approximately

$$H_p = \frac{\eta_b(HV)(\dot{m}_f/\dot{m}_a) + H_a - Q_t/\dot{m}_a}{(1 + \dot{m}_f/\dot{m}_a)} \quad (5)$$

The quantity H_p is the average enthalpy of the products of combustion after mixing has occurred with the air that bypassed the burner. The burner efficiency η_b depends upon the operating conditions but is generally about 0.96 to 0.98. The heating value of the fuel HV, for methanol, for example, is 170.9 kg-cal/g mol wt (9613 Btu/lb), as given in the *Handbook of Chemistry and Physics*.* The quantity $\dot{m}_f/\dot{m}_a$ is the fuel/air ratio, H_a is the enthalpy of the air stream at the burner inlet, and Q_t represents the heat transferred externally from the air heater. After the enthalpy H_p has been evaluated, the temperature is calculated using the specific heat of the gas stream, or it is obtained from a table of properties.

G. Heat Transfer

Instrumentation is provided for the purpose of acquiring heat-transfer distributions from portions of the air heater and from the nozzle by calorimetry. Multijunc-

*44th Edition, The Chemical Rubber Publishing Company, Cleveland, Ohio, 1963, p. 1931.

tion thermocouples are used to measure the temperature difference directly between the inlet and the outlet tubes of coolant passages. The data are recorded on a multichannel digital recorder. The mass flowrate of the water coolant is obtained with rotameters. The heat transfer over the surface area of each coolant passage is then calculated using the specific heat of the water, the mass flowrate of the water, and the temperature difference.

VIII. Summary

The aerodynamic noise facility at the Jet Propulsion Laboratory was designed to be used primarily for investigating the noise-generating mechanisms of high-temperature supersonic and subsonic jets. It can, however, be used for investigating other sources of noise as well. The facility consists of an anechoic chamber, an exhaust jet silencer, instrumentation equipment, and an air heater with associated fuel and cooling systems. Compressed air, when needed for jet noise studies, is provided by the wind tunnel compressor facility.

The interior surfaces of the walls, the ceiling, and the floor of the anechoic room are lined with fiberglass wedge blocks. Between the tips of the wedge blocks, the chamber is 8.1 m long, 5.0 m wide, and 3.0 m high. A spring-loaded wire cable floor, woven with a 5×5 cm mesh, provides the support for personnel walking inside the chamber. Provisions have been made for allowing outside air to be drawn into the anechoic chamber between the wedge blocks in order to replenish the air that is entrained by the jet as it flows through the chamber. Also, openings are provided in the walls and in the ceiling for the purpose of acquiring optical measurements with the use of crossed laser beams. In addition, photographs of the flow field can be taken using a Schlieren or a Shadowgraph system. The chamber is calibrated for noise reflections from the wall in octave bands between 31.2 Hz and 32 kHz. There is a comparatively large region in the chamber where the departure from an inverse square relationship for radiated noise in octave bands between 250 Hz and 16 kHz is comparatively small (between 0 and 1 dB). At lower frequencies, this region is smaller because of a design limitation on the wedge blocks, and at 32 kHz, the departure from an inverse square is larger because of the attenuation of sound in air. The calibrations were made in sufficient detail so that corrections could be made to the experimental measurements.

The inlet of the jet silencer, which is located at the opposite end of the room from the supersonic nozzle, is 2.06 m in diameter. The inlet section is adjustable in the streamwise direction and can be extended into the chamber as much as 1.5 m in order to capture comparatively large jets. The purpose of the silencer is to attenuate the noise radiated to the surrounding area after the jet has passed through the chamber. Experiments have indicated that the attenuation of jet noise by the silencer in terms of sound pressure level ranged from about 35 to 55 dB over the broad frequency band range.

The compressed air supply can be heated by means of fuel-air combustion over a range of temperatures up to approximately 1640 K (2500°F). The maximum operating pressure is 35.1 kg/cm^2 (500 psia), and the maximum available compressed air flowrate on a continuous basis is about 6.4 kg/s (14 lb/s).

The spectral distribution of the sound pressure levels can be obtained by means of microphones. A method using cross correlations has been developed for evaluating the noise spectrum in the moving reference frame for noise sources that move, as, for example, in a jet.

A cross-correlation method has also been developed for experimentally evaluating density fluctuations of the noise sources (eddies) in the moving reference frame of the eddy motion in a high-temperature jet flow by the use of crossed laser beams set up as a Schlieren system. In addition, the convection velocity of the eddies can be evaluated by displacing one of the beams along the jet axis and delaying the signal from the upstream beam.

Additional instrumentation is available for evaluating the thrust of the nozzle, mean velocity, pressure, and temperature distributions in a high-temperature jet flow, by use of wall pressure taps.

Nomenclature

A	local cross-sectional area
C_D	flow coefficient
H_a	enthalpy of air entering air heater
H_p	enthalpy of products of combustion
HV	heating value of fuel
$\dot{m}$	mass flowrate
p	sound pressure level
p'	measured sound pressure level
p_t	stagnation pressure
Q_t	heat-transfer rate (heat loss from air heater)
R	gas constant
r, r_0	distance from noise source
SPL	sound pressure level
T_t	stagnation temperature
γ	specific heat ratio
ϵ	difference between measured and inverse square SPL (Eq. 2)
η_b	burner efficiency

Subscripts

a	air
f	fuel
t	local stagnation condition
th	at the throat
1-D	one-dimensional

NASA — JPL — Coml., L.A., Calif.

N72-30249

TECHNICAL REPORT STANDARD TITLE PAGE

1. Report No. 32-1564	2. Government Accession No.	3. Recipient's Catalog No.
4. Title and Subtitle AN ANECHOIC CHAMBER FACILITY FOR INVESTIGATING AERODYNAMIC NOISE		5. Report Date September 15, 1972 6. Performing Organization Code
7. Author(s) P. F. Massier, S. P. Parthasarathy		8. Performing Organization Report No.
9. Performing Organization Name and Address JET PROPULSION LABORATORY California Institute of Technology 4800 Oak Grove Drive Pasadena, California 91103		10. Work Unit No. 11. Contract or Grant No. NAS 7-100 13. Type of Report and Period Covered Technical Report
12. Sponsoring Agency Name and Address NATIONAL AERONAUTICS AND SPACE ADMINISTRATION Washington, D.C. 20546		14. Sponsoring Agency Code

15. Supplementary Notes

16. Abstract

The aerodynamic noise facility at the Jet Propulsion Laboratory was designed to be used primarily for investigating the noise-generating mechanisms of high-temperature supersonic and subsonic jets. It can, however, be used for investigating other sources of noise as well. The facility consists of an anechoic chamber, an exhaust jet silencer, instrumentation equipment, and an air heater with associated fuel and cooling systems. Compressed air, when needed for jet noise studies, is provided by the wind tunnel compressor facility on a continuous basis.

The chamber is 8.1 m long, 5.0 m wide, and 3.0 m high. Provisions have been made for allowing outside air to be drawn into the anechoic chamber in order to replenish the air that is entrained by the jet as it flows through the chamber. Also, openings are provided in the walls and in the ceiling for the purpose of acquiring optical measurements. Calibration of the chamber for noise reflections from the wall was accomplished in octave bands between 31.2 Hz and 32 kHz.

17. Key Words (Selected by Author(s))	18. Distribution Statement
Acoustics Test Facilities and Equipment Jet Noise	Unclassified -- Unlimited

19. Security Classif. (of this report)	20. Security Classif. (of this page)	21. No. of Pages	22. Price
Unclassified	Unclassified	24	

HOW TO FILL OUT THE TECHNICAL REPORT STANDARD TITLE PAGE

Make items 1, 4, 5, 9, 12, and 13 agree with the corresponding information on the report cover. Use all capital letters for title (item 4). Leave items 2, 6, and 14 blank. Complete the remaining items as follows:

3. Recipient's Catalog No. Reserved for use by report recipients.

7. Author(s). Include corresponding information from the report cover. In addition, list the affiliation of an author if it differs from that of the performing organization.

8. Performing Organization Report No. Insert if performing organization wishes to assign this number.

10. Work Unit No. Use the agency-wide code (for example, 923-50-10-06-72), which uniquely identifies the work unit under which the work was authorized. Non-NASA performing organizations will leave this blank.

11. Insert the number of the contract or grant under which the report was prepared.

15. Supplementary Notes. Enter information not included elsewhere but useful, such as: Prepared in cooperation with... Translation of (or by)... Presented at conference of... To be published in...

16. Abstract. Include a brief (not to exceed 200 words) factual summary of the most significant information contained in the report. If possible, the abstract of a classified report should be unclassified. If the report contains a significant bibliography or literature survey, mention it here.

17. Key Words. Insert terms or short phrases selected by the author that identify the principal subjects covered in the report, and that are sufficiently specific and precise to be used for cataloging.

18. Distribution Statement. Enter one of the authorized statements used to denote releasability to the public or a limitation on dissemination for reasons other than security of defense information. Authorized statements are "Unclassified—Unlimited," "U. S. Government and Contractors only," "U. S. Government Agencies only," and "NASA and NASA Contractors only."

19. Security Classification (of report). NOTE: Reports carrying a security classification will require additional markings giving security and downgrading information as specified by the Security Requirements Checklist and the DoD Industrial Security Manual (DoD 5220.22-M).

20. Security Classification (of this page). NOTE: Because this page may be used in preparing announcements, bibliographies, and data banks, it should be unclassified if possible. If a classification is required, indicate separately the classification of the title and the abstract by following these items with either "(U)" for unclassified, or "(C)" or "(S)" as applicable for classified items.

21. No. of Pages. Insert the number of pages.

22. Price. Insert the price set by the Clearinghouse for Federal Scientific and Technical Information or the Government Printing Office, if known.

floor woven with a 5 × 5 cm mesh, also visible in Figs. 4 and 5, which provides the support for personnel walking inside the chamber, is located 16 cm above the tips of of the wedge blocks that are laid directly on the concrete floor. Numerous stanchion supports are provided, and holes were cut through the wedge blocks so that pipes can easily be attached to the supports, which are mounted on the floor. The stanchions are used to support microphones, as shown in Fig. 5, aerodynamic instrumentation such as pressure and temperature probes, and other instrumentation.

Calibration of the anechoic chamber in terms of sound absorption was accomplished by measuring the sound pressure levels (intensities) at numerous locations, with noise being emitted from a single noise source at a fixed location. In a strictly anechoic chamber, there would be no reflections and the intensity of sound would decrease as the square of the distance from the source (6 dB for every doubling of the distance from the source). However, because of the presence of a silencer that projects a short distance into the room and the lower cutoff frequency of the wedge blocks, reflections do occur to some extent, more at some frequencies than at others. Reflections from the wire-cable floor are negligible at distances of 10 cm or more above the wires.

The noise source used for the calibration was a 15-cm speaker driven by a random noise generator and positioned in the room as shown in Fig. 6, which also shows contours of the overall sound pressure level. The overall intensity, as well as the intensity in octave bands, of the sound emitted was measured with a B&K portable sound level meter. During the measurements, the diaphragm of the speaker was always positioned to be perpendicular to the lines along which measurements were being made (A through I, as indicated in Fig. 6). This eliminated any effects of directionality that the noise emitted by the speaker could have on the sound pressure level (SPL) contours. The lines along which measurements were made were all located in the horizontal plane, passing through the center of the chamber. Data were recorded at distances of 120, 160, 200, 240, 320, 440, 560, and 680 cm from the speaker. From these measurements, contours of equal sound pressure in decibels were constructed for each octave band. The results are shown in Figs. 7 through 17. In a chamber that is perfectly anechoic, these contours would be circles centered at the speaker; thus, departures from circles indicate that reflections exist. Also, in an ideal anechoic chamber, the SPL in any octave band can be evaluated by the equation

$$p(r) = p(r_0) - 20 \log_{10}\left[\frac{r}{r_0}\right] \tag{1}$$

where r and r_0 are the distances from the source.* If the measured SPL is denoted as $p'(r)$, then a measure of the quality of the chamber is indicated by the departure from the inverse square relationship of Eq. (1), which will be denoted as ϵ. Thus,

$$\epsilon = p'(r) - p(r) \tag{2}$$

Substituting Eq. (1) into Eq. (2) gives

$$\epsilon = p'(r) - \left\{p(r_0) - 20 \log_{10}\left[\frac{r}{r_0}\right]\right\} \tag{3}$$

If it is assumed that $p'(r_0) = p(r_0)$ at r_0 close to the source, the values of ϵ can be obtained from the measurements. These values of ϵ are given in Tables 1 through 9.

It is seen from the tables that ϵ is comparatively large ($|\epsilon| > 2$) and negative in the 32-kHz band. The reason for this is attenuation of sound in air, which can be about 1 dB/m at 30 kHz; thus, measured values are less than the inverse square relationship, as indicated by the negative sign, and increase negatively with distance. At intermediate frequencies, the departure from an inverse square distribution is smaller. Then, at the low end of the spectrum (e.g., 31 and 62 Hz and, to a smaller extent, in the 125-Hz band), the value of ϵ is again comparatively large. In this range, the fiberglass wedges do not absorb sound as well because of their low-frequency design limitation, and reflections occur which can make the values of ϵ either positive or negative. There is a comparatively large region in the anechoic chamber that extends downstream from the nozzle (or speaker) where ϵ is low (0 to 1 dB), and this is where most of the jet noise measurements are made. Along the direction of maximum emission from the jet (i.e., along lines B, C, G, and H) ϵ is small over a large part of the distance from the speaker.

The value of ϵ is larger along lines B and C because the booms which support the microphones for the jet noise experiments were present during these tests, whereas there were no such supports on the other side of the chamber. These booms are wrapped with fiberglass that is 5 cm thick; nevertheless, they do reflect somewhat at the lower frequencies. Regions in which ϵ varies between various limits are shown in Fig. 18.

*Parentheses denote "function of" in all of the equations.